Int. J. Heat Mass Transfer. Vol. 36, No. 15, pp. 3851–3857, 1993
Printed in Great Britain

0017-9310/93 $6.00+0.00

Transient behaviour analysis of a latent heat thermal storage module

C. BELLECCI
Dipartimento di Fisica, Universita' della Calabria, 87030 Rende, Italy

and

M. CONTI
Dipartimento di Matematica e Fisica, Universita' di Camerino, 62032 Camerino, Italy

(*Received* 7 *December* 1992)

Abstract—The transient behaviour of a latent heat thermal storage module has been simulated numerically by the enthalpy method in a two-dimensional approximation. Standard experimental correlations were utilized to model the forced convective heat charge and extraction. A parametric study on the performances of the storage module has been conducted; the results are presented and discussed.

INTRODUCTION

THE UTILIZATION of solar energy for dynamic power generation is a matter of growing interest due to the space applications perspectives [1, 2]. For this purpose, some provision of thermal storage becomes quite necessary in order to bridge the eclipse phases. Latent heat thermal storage in a solid–liquid phase change has been proved an interesting method on account of the high storage density and the isothermal nature of the storage and recovery processes [3, 4].

A latent heat thermal storage module (TSM) is shown in Fig. 1. A tube is surrounded by an external coaxial cylinder; the annular gap is filled with a phase change material (PCM). A fluid flows through the inner tube and exchanges heat along the way. During the active phase the PCM melts; the heat conveyed by the hot fluid is partly stored in the phase transition of the PCM and is partly supplied to the heat engine. During the eclipse, the PCM solidifies and the stored latent heat is delivered to the cold fluid.

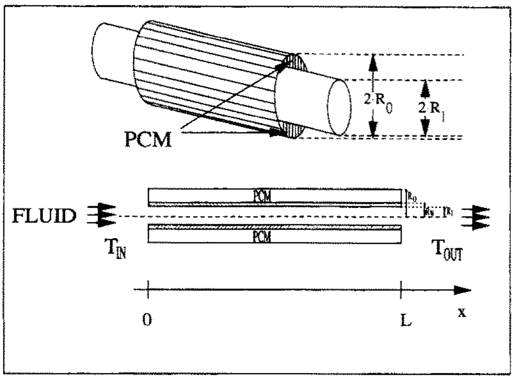

FIG. 1. Thermal storage module (TSM).

The numerical description of the TSM performances cannot be reduced to a simple solution of the Fourier equation, because inside the PCM the melting front moves continuously with time and its position is a priori unknown.

A similar problem was modelled by Cao and Faghri [5]. They attempted to optimize the geometry of the TSM by examining the energy storage process alone. In practice, however, these systems are operated in a cyclic manner, a single cycle consisting of a storage process followed by a removal process. Failure to account correctly for this aspect can lead to a significant error for the evaluation of the system performances. In their numerical study, the fluid flow and the heat diffusion inside the PCM were solved simultaneously as a conjugate problem. However, it has been shown [6] that in normal operative conditions the forced convective heat transfer in the inner tube can be accurately described through standard experimental correlations. This allows us to treat the fluid velocity as an independent variable and to drop the continuity and momentum equations: a dramatic simplification of the problem is then achieved.

In this paper, the transient behaviour of the TSM shown in Fig. 1 has been simulated in a multiple cycle operation, until steady reproducibility is attained. The duration of the sunlight and the eclipse phases is representative for low earth orbit space applications. The forced convection in the inner tube has been treated through an experimental correlation. The standard enthalpy method [7–11] has been utilized to describe the heat diffusion inside the PCM. The resulting equations have been solved numerically by the finite-difference method. The model has been utilized to show the influence of some design parameters on the performances of the TSM.

NOMENCLATURE

c specific heat capacity
D inner diameter of the TSM
F nondimensional storage density, as defined in equation (9)
h convective heat transfer coefficient
H enthalpy per unit volume
H^* nondimensional enthalpy, $H^* = (H - \rho_S c_S T_M)/(\rho_L \lambda)$
$\bar{H}$ enthalpy stored in the PCM, as defined in equation (10)
k thermal conductivity
L length of the TSM
M PCM mass
Nu Nusselt number, defined as $D h/k_F$
Pe Peclet number, $Pe = Re\, Pr$
Pr Prandtl number, defined as $c_F \mu/k_F$
Q^* $T_M/(T_C - T_M)$
r_I, r_O inner and outer radius of the TSM, respectively
r_W radius at the wall PCM interface
Re Reynolds number, defined as $D \rho_F v/\mu$
St Stefan number, defined as $c_L (T_C - T_M)/\lambda$
t time
t_C duration of a full sunlight–eclipse cycle
t_{ECL} duration of the eclipse phase in a cycle
t_{SUN} duration of the sunlight phase in a cycle
T_0 initial temperature of the TSM
T_C inlet fluid temperature (charge phase)
T_R inlet fluid temperature (removal phase)
T_{OUT} fluid temperature at the outlet of the TSM
T_M melting temperature of the PCM
T temperature [K]
T^* nondimensional temperature, $(T - T_M)/(T_C - T_M)$
v fluid velocity
x, r axial and radial coordinates, respectively.

Greek symbols
α thermal diffusivity
λ latent heat of the PCM
μ fluid viscosity
ξ, η nondimensional coordinates, x/D, r/D, respectively
ρ density
τ nondimensional time, $(\rho_F c_F/\rho_L c_L)$ $[c_L (T_C - T_M)/\lambda]$ (v/D) t
τ_C nondimensional cycle period, $(\rho_F c_F/\rho_L c_L)$ $[c_L (T_C - T_M)/\lambda]$ (v/D) t_C
χ k_S/k_L.

Subscripts
F fluid
L liquid phase of the PCM
MIN minimum value
MAX maximum value
P PCM
S solid phase of the PCM
W walls.

THE MATHEMATICAL MODEL

The numerical calculations have been conducted under the following assumptions:

- the heat transfer fluid is incompressible and viscous heating is neglected;
- the fluid flow is radially uniform, and the axial velocity is an independent parameter;
- heat diffusion in the containment walls is considered only at the fluid–PCM interface, i.e. zero thickness of the outer walls is assumed;
- no thermal losses through the outer walls;
- heat diffusion inside the TSM is axisymmetric;
- equal duration of the sunlight and the eclipse phase, $t_{SUN} = t_{ECL} = t_C/2$;
- no natural convection inside the liquid PCM (microgravity conditions); and
- convective terms due to contractions and expansions of the PCM in the phase change are neglected.

The energy equations governing the heat transfer inside the storage module, written for the fluid, the pipe walls and the PCM are

Fluid

$$\frac{\partial H_F}{\partial t} + \rho_F c_F v \frac{\partial T_F}{\partial x} = \frac{4h}{D}[T_W(r = r_I) - T_F] + k_F \frac{\partial^2 T_F}{\partial x^2} \tag{1}$$

Walls

$$\frac{\partial H_W}{\partial t} = \frac{1}{r}\frac{\partial}{\partial r}\left(k_W r \frac{\partial T_W}{\partial r}\right) + \frac{\partial}{\partial x}\left(k_W \frac{\partial T_W}{\partial x}\right) \tag{2}$$

PCM

$$\frac{\partial H_P}{\partial t} = \frac{1}{r}\frac{\partial}{\partial r}\left(k_P r \frac{\partial T_P}{\partial r}\right) + \frac{\partial}{\partial x}\left(k_P \frac{\partial T_P}{\partial x}\right). \tag{3}$$

H in equations (1)–(3) indicates the enthalpy per unit volume and is related to the temperature via

$$T = A\,H + B \tag{4}$$

where

Fluid

$$A = \frac{1}{(\rho_F c_F)}; \quad B = 0$$

Walls

$$A = \frac{1}{(\rho_W c_W)}; \quad B = 0$$

PCM

$$A = \frac{1}{(\rho_S c_S)}; \quad B = 0 \quad (H_P < \rho_S c_S T_M)$$

$$A = 0; \quad B = T_M \quad \left(0 \leqslant \frac{(H_P - \rho_S c_S T_M)}{\rho_L \lambda} \leqslant 1\right)$$

$$A = \frac{1}{(\rho_L c_L)}; \quad B = T_M\left(1 - \frac{\rho_S c_S}{\rho_L c_L}\right) - \frac{\lambda}{c_L} \quad \left(\frac{H_P - \rho_S c_S T_M}{\rho_L \lambda} > 1\right).$$

The initial and boundary conditions for equations (1)–(3) are specified by

initial conditions

$$T = T_0 \quad 0 \leqslant r \leqslant r_O; \quad 0 \leqslant x \leqslant L$$

boundary conditions

$$T = T_C \text{ (storage)} \quad x = 0; \quad 0 \leqslant r \leqslant r_I$$

$$T = T_R \text{ (removal)} \quad x = 0; \quad 0 \leqslant r \leqslant r_I$$

$$\frac{\partial T}{\partial x} = 0 \quad x = 0; \quad r_I \leqslant r \leqslant r_O$$

$$\frac{\partial T}{\partial x} = 0 \quad x = L; \quad 0 \leqslant r \leqslant r_O$$

$$h(T_W - T_F) = k_W \frac{\partial T_W}{\partial r} \quad 0 \leqslant x \leqslant L; \quad r = r_I$$

$$k_W \frac{\partial T_W}{\partial r} = k_P \frac{\partial T_P}{\partial r} \quad 0 \leqslant x \leqslant L; \quad r = r_W$$

$$\frac{\partial T_P}{\partial r} = 0 \quad 0 \leqslant x \leqslant L; \quad r = r_O.$$

The initial temperature T_0 of the TSM is assumed to be uniform and the PCM is in the solid phase. The working fluid enters into the TSM at a constant temperature during each phase.

The problem can be conveniently reformulated in terms of the following nondimensional variables

$$\eta = r/D; \quad \xi = x/D; \quad \tau = \frac{\rho_F c_F}{\rho_L c_L} \frac{c_L (T_C - T_M)}{\lambda} \frac{v}{D} t$$

$$T^* = (T - T_M)/(T_C - T_M);$$

$$H^* = (H - \rho_S c_S T_M)/(\rho_L \lambda)$$

$$St = c_L (T_C - T_M)/\lambda; \quad Q^* = T_M/(T_C - T_M)$$

$$\chi = k_P/k_L; \quad \tau_C = \frac{\rho_F c_F}{\rho_L c_L} \frac{c_L (T_C - T_M)}{\lambda} \frac{v}{D} t_C.$$

The dimensionless energy equations can be written as follows

Fluid

$$\frac{\partial H_F^*}{\partial \tau} + \frac{\partial T_F^*}{\partial \xi} = 4 \frac{Nu}{Re\, Pr}(T_W^* - T_F^*) + \frac{1}{Re\, Pr} \frac{\partial^2 T_F^*}{\partial \xi^2} \tag{5}$$

Walls

$$\frac{\partial H_W^*}{\partial \tau} = \frac{k_W}{k_F} \frac{1}{Re\, Pr}\left(\frac{\partial^2 T_W^*}{\partial \xi^2} + \frac{1}{\eta} \frac{\partial}{\partial \eta} \eta \frac{\partial T_W^*}{\partial \eta}\right) \tag{6}$$

PCM

$$\frac{\partial H^*}{\partial \tau} = \frac{k_L}{k_F} \frac{1}{Re\, Pr}\left(\frac{\partial}{\partial \xi} \chi \frac{\partial T^*}{\partial \xi} + \frac{1}{\eta} \frac{\partial}{\partial \eta} \chi \eta \frac{\partial T^*}{\partial \eta}\right). \tag{7}$$

The initial and boundary conditions are specified as follows

initial conditions

$$T^* = T_0^* \quad 0 \leqslant \eta \leqslant r_O/D; \quad 0 \leqslant \xi \leqslant L/D$$

boundary conditions

$$T^* = 1 \text{ (storage)} \quad \xi = 0; \quad 0 \leqslant \eta \leqslant 0.5$$

$$T^* = T_R^* \text{ (removal)} \quad \xi = 0; \quad 0 \leqslant \eta \leqslant 0.5$$

$$\frac{\partial T^*}{\partial \xi} = 0 \quad \xi = 0; \quad 0.5 \leqslant \eta \leqslant r_O/D$$

$$\frac{\partial T^*}{\partial \xi} = 0 \quad \xi = L/D; \quad 0 \leqslant \eta \leqslant r_O/D$$

$$\frac{1}{Nu} \frac{k_W}{k_F} \frac{\partial T_W^*}{\partial \eta} = (T_W^* - T_F^*) \quad 0 \leqslant \xi \leqslant L/D; \quad \eta = 0.5$$

$$\frac{\partial T_W^*}{\partial \eta} = \chi \frac{k_L}{k_F}\left(\frac{k_W}{k_F}\right)^{-1} \frac{\partial T_P^*}{\partial \eta} \quad 0 \leqslant \xi \leqslant L/D; \quad \eta = r_W/D$$

$$\frac{\partial T_P^*}{\partial \eta} = 0 \quad 0 \leqslant \xi \leqslant L/D; \quad \eta = r_O/D.$$

The nondimensional enthalpy is related to the temperature via

$$T^* = A^* H^* + B^* \tag{8}$$

where

Fluid

$$A^* = \frac{1}{St}\left(\frac{\rho_F c_F}{\rho_L c_L}\right)^{-1}; \quad B^* = Q^*\left[\frac{\rho_S c_S}{\rho_L c_L}\left(\frac{\rho_F c_F}{\rho_L c_L}\right)^{-1} - 1\right]$$

Walls

$$A^* = \frac{1}{St}\left(\frac{\rho_W c_W}{\rho_L c_L}\right)^{-1};$$

$$B^* = Q^*\left[\frac{\rho_S c_S}{\rho_L c_L}\left(\frac{\rho_W c_W}{\rho_L c_L}\right)^{-1} - 1\right]$$

PCM

$$A^* = \frac{1}{St}\left(\frac{\rho_S c_S}{\rho_L c_L}\right)^{-1}; \quad B^* = 0 \quad (H^* < 0)$$

$$A^* = 0; \quad B^* = 0 \quad (0 \leqslant H^* \leqslant 1)$$

$$A^* = \frac{1}{St}; \quad B^* = -\frac{1}{St} \quad (H^* > 1).$$

It can be observed that the temperature field in the TSM depends on

$$\tau, \ \tau_C, \ St, \ Q^*, \ \frac{\rho_S c_S}{\rho_L c_L}, \ \frac{\rho_F c_F}{\rho_L c_L}, \ \frac{\rho_W c_W}{\rho_L c_L}, \ Nu,$$

$$Pe, \ \frac{k_W}{k_F}, \ \frac{k_L}{k_F}, \ \chi,$$

$$T_0^*, \ T_R^*, \ r_O/D, \ r_W/D, \ L/D.$$

Equations (5)–(7) have been approximated with the control–volume finite-difference approach suggested by Patankar [12, 13]. The resulting algebraic equations were solved by the tridiagonal matrix algorithm. Due to the intrinsic nonlinearity of the problem, some iterations were needed at each time step. Convergence was assumed when the values of all the variables were stabilized within 0.1%.

The consistency of the computational scheme has been checked by performing an overall energy balance at each time step: energy is conserved within 0.01% of the total heat delivered to (or removed from) the PCM.

NUMERICAL RESULTS

The lack of experimental data makes it difficult to validate the present model. However, some significative results have been checked against the numerical solution by Cao and Faghri [5] for the charge phase alone. The comparison is shown in Fig. 2 where the melting front position is shown at different times. The dimensionless parameters that characterize

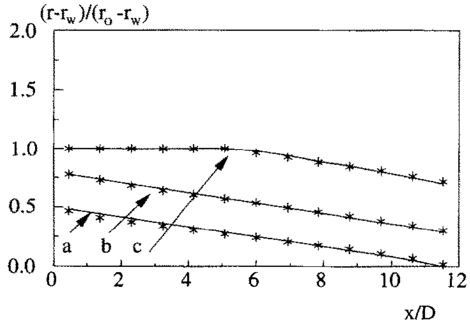

FIG. 2. Melting front positions at different times. Curve (a) $vt/D = 150$; curve (b) $vt/D = 400$; curve (c) $vt/D = 1000$. Lines: as calculated by Cao and Faghri [5]; asterisks: present study. The set of nondimensional parameters that characterizes the solution is specified in Table 1.

Table 1. Values of the dimensionless parameters that characterize the solution shown in Fig. 2

Re	2200
Pr	0.0065
$c_L(T_{IN}-T_M)/\lambda$	0.5
$(T_0-T_M)/(T_{IN}-T_M)$	−0.1
c_S/c_L	1
k_S/k_L	1
α_L/α_F	0.02
α_W/α_F	0.11
k_F/k_W	1.42
k_L/k_W	0.124
r_O/D	1.325
r_W/D	0.575
L/D	12

the solution according to the choice of Cao and Faghri are specified in Table 1. The Nusselt number in equation (5) has been obtained from the numerical results of Chen and Chiou for liquid metals in the thermal and velocity entry length region [14]. It can be observed from the figure that the agreement is quite satisfactory. It is worth noting that the very small L/D ratio that is utilized is quite unrealistic from a technical point of view; at higher values of L/D the entry length effects lose their importance and the present model should operate even better.

The model has been utilized to show the influence of the geometrical features on the performances of the TSM in a multiple cycle operation.

Moreover, a central point in this respect is the duration of the eclipse phase, i.e. the timing of the charge-removal processes. This effect has been investigated too. Sodium has been chosen as the working fluid; the PCM is an eutectic mixture of LiF–MgF_2, characterized by a high heat of fusion and a melting temperature suited for power production applications. The thermophysical properties of the PCM are referenced in [15] and summarized in Table 2. Table 3 shows the values of the nondimensional parameters that have been utilized in this investigation.

Two leading criteria underlie an efficient design of the storage module:

(i) the oscillations of the fluid outlet temperature in the charge-removal cycles should be kept in a narrow range; and

(ii) high storage density is required, especially in space-based applications.

Figure 3 shows, vs r_O/D, the maximum and minimum values of T^*_{OUT} in a full charge-removal process. The

Table 2. Thermophysical properties of the PCM

T_M	1008 K
λ	550 000 J kg^{-1}
ρ_L	2300 kg m^{-3}
ρ_S	2630 kg m^{-3}
c_L	1990 J kg^{-1} K^{-1}
c_S	2510 J kg^{-1} K^{-1}
k_P	3.5 W m^{-1} K^{-1}

Table 3. Values of the dimensionless parameters utilized in the present paper

St	0.579
Q^*	6.30
$\frac{\rho_S c_S}{\rho_L c_L}$	1.44
$\frac{\rho_F c_F}{\rho_L c_L}$	0.213
$\frac{\rho_W c_W}{\rho_L c_L}$	0.785
Pe	7.56
k_W/k_F	0.740
k_L/k_F	5.86×10^{-2}
χ	1
T_0^*	0
T_R^*	-1
r_W/D	0.575

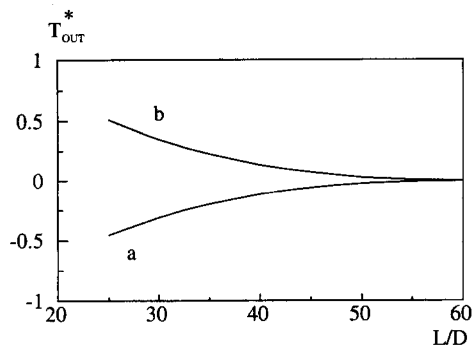

FIG. 4. Fluid temperature at the outlet of the TSM vs L/D. $\tau_C = 800$; $r_O/D = 1.5$. Curves (a) and (b) represent the minimum and the maximum values, respectively, in a steady cycle. The other nondimensional parameters that characterize the solution are specified in Table 3.

results refer to a steady operation, after the start-up effects have died out: this condition is generally attained within the first five cycles even at large r_O/D. We can observe that increasing the external radius of the TSM results in high stability of the fluid outlet temperature; the drawback is due to the increase of the storage mass. However, the figure shows that poor improvement in the T^*_{OUT} stability is attained for $r_O/D > 1.6$—this is a useful indication for a proper selection of the TSM radial size. Figure 4 shows the effect of different L/D: the T^*_{OUT} stability increases with L/D. Here, too, the need to quench the T^*_{OUT} oscillations contrasts with the requirement of low storage mass.

The timing of the charge-removal process affects the TSM performances. Figure 5 shows the maximum and minimum values of T^*_{OUT} vs the nondimensional cycle duration τ_C. It is worth observing that τ_C embodies the fluid flow-rate and its order of magnitude is the ratio of the heat discharged by the fluid in a cycle to the total heat of fusion of the PCM. As it can be expected, better T^*_{OUT} stability is attained when over-loading as well as exhaustion of the storage module is prevented, i.e. for low cycle duration.

A better understanding of the problem can be achieved if we note that for an efficient operation of the thermal storage, heat must be stored as latent heat in the phase change; overheating as well as subcooling of the PCM must be avoided. The problem can be conveniently stated in terms of a nondimensional storage density, defined as

$$F = \frac{\bar{H}}{M\lambda} \tag{9}$$

where $\bar{H}$ represents the enthalpy stored in the PCM

$$\bar{H} = \int_{V_{PCM}} (H - \rho_S c_S T_M)\,dx\,dy\,dz. \tag{10}$$

F represents the ratio of the enthalpy stored in the PCM to the total heat of fusion of PCM utilized.

If in a cycle it results $F_{MIN} < 0$ and/or $F_{MAX} > 1$

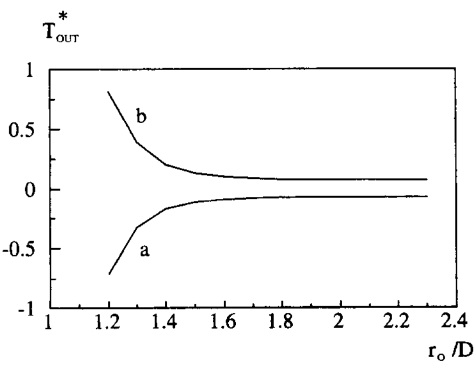

FIG. 3. Fluid temperature at the outlet of the TSM vs r_O/D. $L/D = 40$; $\tau_C = 800$. Curves (a) and (b) represent the minimum and the maximum values, respectively, in a steady cycle. The other nondimensional parameters that characterize the solution are specified in Table 3.

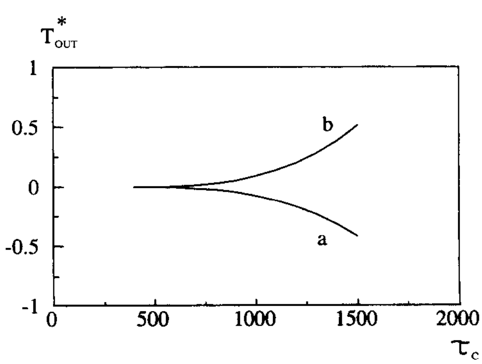

FIG. 5. Fluid temperature at the outlet of the TSM vs τ_C; $r_O/D = 1.5$; $L/D = 40$. Curves (a) and (b) represent the minimum and the maximum values, respectively, in a steady cycle. The other nondimensional parameters that characterize the solution are specified in Table 3.

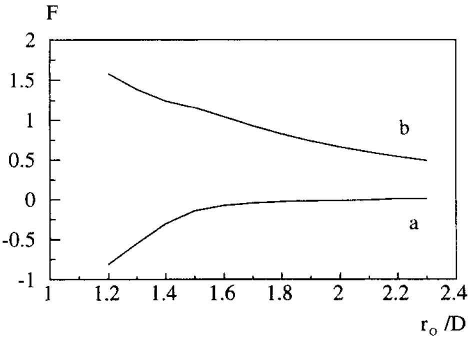

FIG. 6. F values vs r_O/D. F is defined by equation (9). Curves (a) and (b) represent the minimum and maximum values, respectively in a steady cycle. $L/D = 40$; $\tau_C = 800$. The other nondimensional parameters that characterize the solution are specified in Table 3.

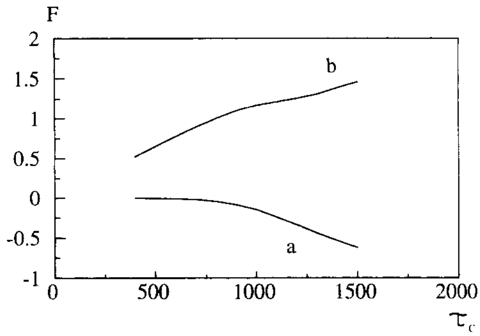

FIG. 8. F values vs the nondimensional cycle period. F is defined by equation (9). Curves (a) and (b) represent the minimum and maximum values, respectively, in a steady cycle. $r_O/D = 1.5$; $L/D = 40$. The other nondimensional parameters that characterize the solution are specified in Table 3.

subcooling and/or overheating occurs and T^*_{OUT} runs away.

On the other side, it can result in $F_{MIN} > 0$ and/or $F_{MAX} < 1$; it means that only a fraction of the PCM is involved in the phase change.

In a proper design of the thermal storage F should not deviate too much from the range between 0 and 1.

Figure 6 shows the maximum and minimum values of F in a steady cycle vs r_O/D. As expected, the excursions of F decrease as r_O/D increases. The curves indicate that heavy sensible heat operation occurs at $r_O/D < 1.5$; furthermore, the graph shows that for $r_O/D > 2$, a considerable amount of the PCM is excluded from the phase change.

The effect of the TSM length is shown in Fig. 7. At low L/D overheating and subcooling inside the PCM cannot be prevented. A proper selection of the L/D ratio should be in the range 45–55.

Figure 8 illustrates the effect of the timing of the charge-removal processes. It can be observed that overloading and exhaustion of the TSM occurs at $\tau_C > 0.8$; at lower values of τ_C, however, only a small fraction of the PCM is involved in the phase change.

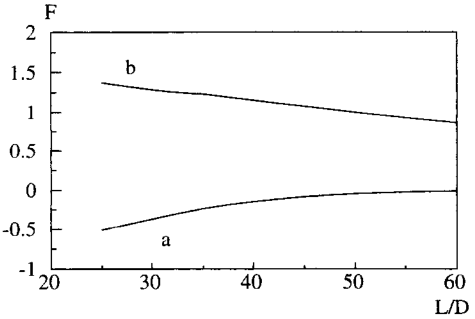

FIG. 7. F values vs L/D. F is defined by equation (9). Curves (a) and (b) represent the minimum and maximum values, respectively, in a steady cycle. $r_O/D = 1.5$; $\tau_C = 800$. The other nondimensional parameters that characterize the solution are specified in Table 3.

CONCLUSIONS

Solar dynamic power generation is attractive for space-based applications, and phase change thermal storage is an effective solution to ensure stability of the thermal power delivered as well as of the operating temperatures. A numerical model has been presented to simulate the cyclic behaviour of a latent heat thermal storage module. The phase change process has been treated by the enthalpy method; the convective heat extraction has been conveniently described in terms of standard heat transfer correlations.

Economy in the storage mass and size must be pursued, but this condition contrasts with the exigency of an adequate stability of the fluid outlet temperature. The numerical results indicate some useful criteria for a convenient compromise in this respect.

REFERENCES

1. H. J. Strumpf and M. G. Coombs, Solar receiver for the space station Brayton engine, *J. Engng Gas Turbines Pwr* **110,** 295 (1988).
2. H. J. Strumpf and M. G. Coombs, Solar receiver experiment for the space station FREEDOM Brayton engine, *J. Solar Energy Engng* **112,** 12 (1990).
3. R. A. Crane and G. Bharadhwaj, Evaluation of thermal energy storage devices for advanced solar dynamic systems, *J. Solar Energy Engng* **113,** 138 (1991).
4. T. K. Stovall and R. V. Arimilli, Transient thermal analysis of three fast-charging latent heat storage configurations, *J. Thermophys. Heat Transfer* **6,** 152 (1992).
5. Y. Cao and F. Faghri, Performance characteristics of a thermal energy storage module: a transient PCM/forced convection conjugate analysis, *Int. J. Heat Mass Transfer* **34,** 93 (1991).
6. C. Bellecci and M. Conti, Phase change thermal storage: transient behaviour analysis of a solar receiver/storage module using the enthalpy method, *Int. J. Heat Mass Transfer* **36,** 2157 (1993).
7. R. M. Furzeland, A comparative study of numerical methods for moving boundary problems, *J. Inst. Math. Appl.* **26,** 411 (1980).
8. V. Voller and M. Cross, Accurate solutions of moving boundary problems using the enthalpy method, *Int. J. Heat Mass Transfer* **24,** 545 (1981).
9. F. Civan and C. M. Sliepcevich, Efficient numerical solu-

tion for enthalpy formulation of conduction heat transfer with phase change, *Int. J. Heat Mass Transfer* **27**, 1428 (1984).
10. Y. Cao, A. Faghri and W. S. Chang, A numerical analysis of Stefan problems for generalized multi-dimensional phase-change structures using the enthalpy transforming model, *Int. J. Heat Mass Transfer* **32**, 1289 (1989).
11. D. B. Duncan, A simple and effective self-adaptive moving mesh for enthalpy formulations of phase change problems, *IMA J. Numer. Analysis* **11**, 55 (1991).
12. S. V. Patankar, *Numerical Heat Transfer and Fluid Flow*. Hemisphere, Washington, D.C. (1980).
13. S. V. Patankar, Elliptic systems: finite difference method I. In *Handbook of Numerical Heat Transfer* (Edited by W. J. Minkowycz *et al.*), pp. 215–290. Wiley, New York (1988).
14. Ching-Jen Chen and Jenq Shing Chiou, Laminar and turbulent heat transfer in the pipe entrance region for liquid metals, *Int. J. Heat Mass Transfer* **24**, 1179 (1981).
15. S. Weingartner and J. Blumenberg, Ceramic materials for space station's heat of fusion thermal energy storage, *41st Congress of the International Astronautical Federation, Dresden, Germany*, 6–12 October 1990, IAF-90-221.